Analysis of the Structural Parameters of Polyacrylonitrile Fibers Containing Nanohydroxyapatite

Teresa Mikołajczyk,[1] Stanisław Rabiej,[2] Maciej Boguń[1]

[1]*Department of Man-Made Fibers, Faculty of Textile Engineering and Marketing, Technical University of Łódź, Łódź, Poland*
[2]*Institute of Polymer Materials and Textile Engineering, Faculty of Textile Engineering and Environmental Protection, University of Bielsko–Biała, Bielsko–Biała, Poland*

Received 6 July 2005; accepted 1 December 2005
DOI 10.1002/app.23978
Published online in Wiley InterScience (www.interscience.wiley.com).

ABSTRACT: The structural parameters and strength properties of a new generation of polyacrylonitrile fibers have been analyzed. These fibers, after being carbonized, can be used in biomaterial engineering. They are characterized by a high tensile strength of 31–43 cN/tex. An advantageous influence of nanoparticles added to the fiber matter on the degree of crystallinity has been found. When nanoparticles of hydroxyapatite are incorporated into these fibers, their degree of crystallinity increases by about 5%.
 J Appl Polym Sci 101: 760–765, 2006

Key words: fibers; orientation; crystal structures; nanoparticles; hydroxyapatite

INTRODUCTION

Carbon composites based on carbon fibers are among the most common materials used in biomaterial engineering. Such composites have found wide applications in many medical fields, such as orthopedics and traumatic surgery, in which they are used in the reconstruction of knee joints[1,2] and Achilles tendons.[3]

The incorporation of a biologically active compound, such as hydroxyapatite (Hap), into precursor polyacrylonitrile (PAN) fibers makes it possible to prepare carbon fibers with new, incomparable properties. A biocomposite made from carbon fibers containing nanoparticles of Hap can become an alternative to other materials used currently in orthopedics and traumatic surgery. The reason for using active Hap as a biologically active compound is that it is one of the most common bioceramic materials[4] used for top layers of titanium implants.[5] Its main advantage, however, is that it is very similar to the inorganic part of bony tissue.[6]

Thus, carbon fibers prepared from a PAN precursor containing nano-Hap will be designed for implants that include in their structure elements with osteoconductive and osteoproductive effects.

If carbon fibers are to be used for implant preparation, they should possess not only appropriate biological properties but also high strength and increased porosity. Both the strength and porosity of carbon fibers depend directly on the structure of the precursor fibers created during their solidification and the subsequent drawing process.[7–9] There is also an inverse effect of the spinning parameters on both these properties.[10] It has been stated that the incorporation of 3–5% SiO_2 nanoparticles into the fiber-forming polymer results in increased fiber porosity and decreased strength, in comparison with fibers spun under the same conditions but without any addition of nanoparticles.[11]

The main aim of investigations into obtaining PAN precursor fibers, which include biologically active Hap, is such a parameter selection of the fiber-formation process, which would secure obtaining fibers of a strength appropriate for carbonization and, at the same time, with increased porosity. This latter parameter is especially important for medical applications of carbon fibers, and it is dependent on the porosity of the precursor fibers.[9] A detailed analysis of the influence of the particular parameters of the fiber-formation process on the porous structure and the properties of PAN fibers with Hap nanoparticles included is presented in our earlier publication.[12]

The aim of this study is to determine the relation between the parameters of the porous and supermolecular structure and the strength properties of precursor PAN fibers with Hap. An analysis carried out by us enables the explanation of why it is possible to obtain PAN fibers with high strength properties, notwithstanding the fact that the fiber polymer matter includes non-fiber-grade nanoparticles.

EXPERIMENTAL

A spinning solution was prepared from a PAN terpolymer, produced by Zoltek (Hungary), with the

Correspondence to: T. Mikołajczyk (mikolter@mail.p.lodz.pl).
Contract grant sponsor: State Committee for Scientific Research; contract grant number: 3T08E03328.

TABLE I
Characteristics of the Polymer and Spinning Solution

Intrinsic viscosity (dL/g)	Concentration of the solution (%)	Hydroxyapatite content (%)	Rheological parameters	
			n	*K*
1.29	22	3	0.955	32.4

n,K = rheological parameters of the model Ostwald de Vaele.

following composition: 93–94 wt % acrylonitrile units, 5–6 wt % methyl acrylate, and about 1 wt % sodium allylsulfonate.

Dimethylformamide (DMF) was used as a solvent.

Hap, delivered by the Academy of Mining and Smelting Engineering (Krakow, Poland), was used in the form of particles with dimensions within the range of 10–100 nm [determined on the basis of scanning electron microscopy (SEM) images].

The characteristics of the spinning solution were determined on the basis of separate measurements,[13] and the results are shown in Table I. The presence of nanoparticles and their distribution in the fiber matter were confirmed on the basis of SEM images and energy-dispersive spectrometry analysis presented in our earlier publication.[12]

Fibers were spun by the wet process from the solution with the use of a laboratory spinning machine that allowed us to stabilize the technological parameters at predetermined levels and under continuous control. A spinneret with 240 orifices, 0.08 mm in diameter each, was used. The solidification process was carried out in a bath containing an aqueous solution of DMF with a concentration in the range of 30–70%. Fibers were drawn in two stages: in a plasticizing bath (containing an aqueous solution of a low DMF concentration) and under superheated steam at a temperature within the range of 110–140°C. After being rinsed, the fibers were dried at 20–40°C under isometric conditions. Precise values of the technological parameters are protected under patent law.[14] The study comprised eight types of Hap-containing PAN fibers processed with various values of the as-spun draw ratio and the total draw ratio (Table I). PAN fibers without the addition of nanoparticles (PW1) were used as reference samples.

The following strength and structural parameters of the fibers were determined: the fiber tenacity, the total orientation coefficient, the degree of crystallinity, and the crystallite dimensions.

The fiber tenacity was determined according to Polish Standard PN-85/P-04761/04 with the use of an Instron tensile testing machine.

The total orientation coefficient was determined by the sonic method. The velocity of wave propagation in the fibers under investigation was measured and related to the wave propagation velocity of isotropic fibers. Measurements were carried out with a PPM-5R dynamic modulus tester from Morgan Co., Inc. (United States).

The degree of crystallinity and the size of the crystallites were determined with the wide-angle X-ray scattering (WAXS) method. Diffraction patterns were recorded in a symmetrical reflection mode with a Seifert URD-6 diffractometer and a copper-target X-ray tube [wavelength (λ) = 1.54 Å] operated at 40 kV and 30 mA. Cu Kα radiation was monochromatized with a Ni filter. WAXS curves were recorded from 6.5 to 60° with a step of 0.1°. The investigated fibers were powdered and pressed into a sample holder. Samples 1 mm thick with a radius of 2 cm were prepared.

RESULTS AND DISCUSSION

The analysis of the WAXS curves and the calculation of the degree of crystallinity were performed with the OptiFit computer program.[15,16] In the first stage, a linear background was determined on the basis of the intensity level at small and large angles and subtracted from the diffraction curve. Moreover, the curves of all samples were normalized to the same value of integral intensity scattered by a sample over the whole range of the scattering angles recorded in the experiment. Next, the experimental diffraction curves were approximated by theoretical curves that were composed of the sum of the functions representing the particular crystalline peaks and the amorphous component. The theoretical curve was fitted to the experimental curve with a multicriterium optimization procedure and a hybrid system that combined a genetic algorithm and a classical optimization method of Powell.[16] Both the crystalline peaks and the amorphous halos were represented by a linear combination of Gauss and Lorentz profiles:

$$F_i(x) = f_i H_i \exp\left\{-\ln 2\left[\frac{2(x - x_{oi})}{w_i}\right]^2\right\} + \frac{(1 - f_i)H_i}{1 + [2(x - x_{oi})/w_i]^2} \quad (1)$$

where x is the scattering angle 2θ, H_i is the peak height, w_i is the width at the half-height, x_{oi} is the peak position, and f_i is the shape factor (f_i = 0 for the Lorentz profile or 1 for the Gauss profile).

The initial values of the crystalline peak positions were calculated from the PAN unit cell dimensions given by Stefani.[17] According to Stefani, the unit cell of PAN is orthorhombic with dimensions of a = 10.2 Å, b = 6.1 Å, and c = 5.1 Å. With these data, the interplanar distances for individual families of lattice planes (d_{hkl}) were calculated:

$$\left(\frac{1}{d_{hkl}}\right)^2 = \left(\frac{h}{a}\right)^2 + \left(\frac{k}{b}\right)^2 + \left(\frac{l}{c}\right)^2 \quad (2)$$

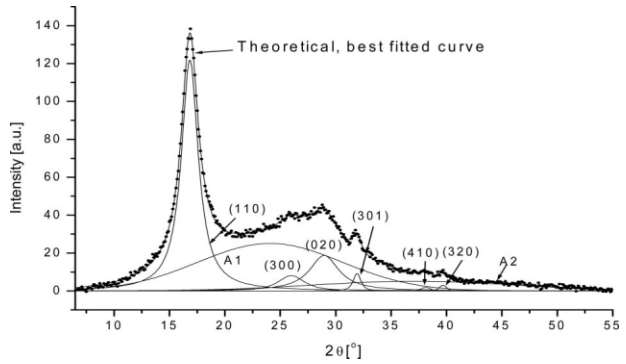

Figure 1 WAXS pattern of a PAN H1 sample resolved into crystalline peaks and amorphous components. The black points are the experimental curve after normalization and background subtraction. A1 and A2 are amorphous maxima.

Next, with Bragg's law, the positions of peaks related to a given family of planes were calculated:

$$2d_{hkl} sin\theta = n\lambda \tag{3}$$

where n is a natural number.

The data related to the unit cell of PAN presented in ref. 18 are considerably differentiated. This is because of the weak and diffuse crystalline peaks of PAN. Moreover, PAN can crystallize in three different polymorphous forms. Calculations performed in this work indicate that the peak positions calculated with the data of Stefani[17] are best fitted to the experimental data obtained by us. The amorphous component was approximated by means of two broad maxima located at $2\theta \approx 24°$, and $2\theta \approx 36°$.

The degree of crystallinity was calculated as the ratio of the total integral intensity of the crystalline peaks to the total integral intensity scattered by a sample over the whole measurement range. Figure 1 presents an example of a WAXS pattern resolved into component parts for a sample containing Hap.

Moreover, Sherrer's formula was used to calculated the size of the crystallites (D_{hkl}) in the direction perpendicular to the family of (110) lattice planes:

$$D_{hkl} = \frac{\lambda}{w\ cos\ \theta} \tag{4}$$

where w is the width at half-height of a peak related to (110) lattice planes. The highest crystalline peak, located at about $2\theta \approx 17°$ in the WAXS pattern of PAN, is related to these planes.

The calculated crystallinity values (Table I and Fig. 2) indicate only a very slight influence of the fundamental technological parameters, such as the as-spun draw ratio and the total draw ratio, on their magnitude. Despite the wide range of changes in these parameters, the crystallinity changes do not exceed 5%. However, the highest values of crystallinity occur for the samples with extreme values of the as-spun draw ratio: −60 and 0.0%. Tempering the solidification process by lowering the temperature and increasing the solvent content in the coagulation bath does not influence significantly the degree of crystallinity either. Its changes do not exceed 5% (Table I). A detailed analysis of the temperature influence on the PAN fiber properties is presented in ref. 12.

A direct comparison of the diffraction patterns for the fibers containing Hap also shows very small differences between them. This fact is illustrated in Figure 3, in which the WAXS curves of two samples with the largest crystallinity difference are presented.

Much better visible differences exist between the WAXS curves of fibers containing Hap and that of the reference sample PW1 with no nanoadditives (Figs. 1 and 4). The differences confirm that Hap affects the

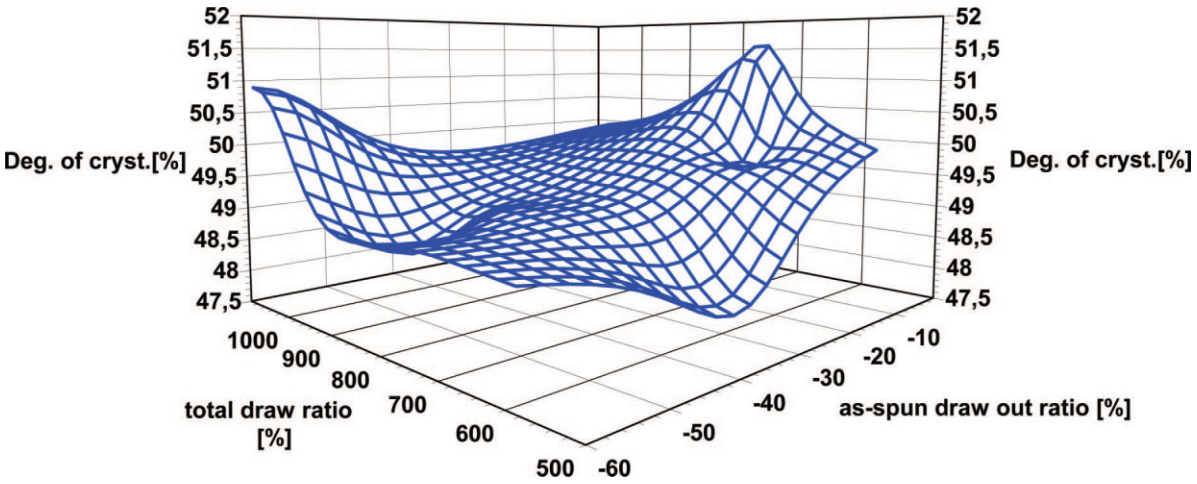

Figure 2 Dependence of the degree of crystallinity on the as-spun draw-out ratio and the total draw ratio for PAN fibers containing Hap. [Color figure can be viewed in the online issue, which is available at www.interscience.wiley.com.]

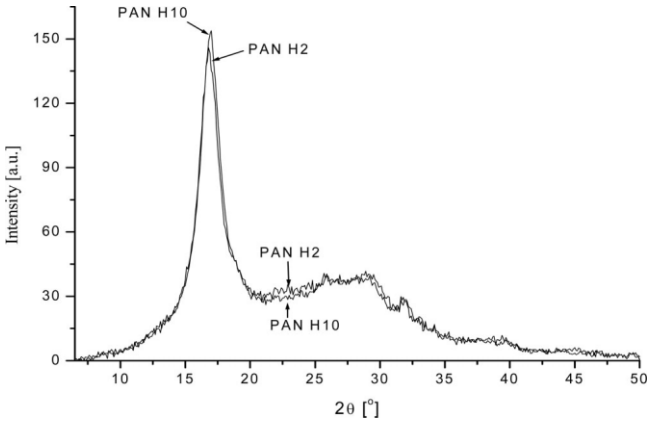

Figure 3 WAXS patterns of two samples containing Hap with the highest (PAN H10, 52%) and lowest (PAN, 47.8%) degree of crystallinity. The figure presents WAXS patterns after background subtraction and normalization.

crystalline structure of the fibers. Despite a relatively small increase in the crystallinity value caused by the presence of Hap, an unambiguous increase can be observed in the average size of the crystallites (Table I) as well as a considerable improvement in the quality and perfection of their crystalline structure. This conclusion results from a comparison of the diffraction patterns recorded for these two types of fibers (Figs. 1 and 4). As is well known, the chains of macromolecules in the regions of PAN called crystalline are in most cases ordered only in the direction perpendicular to their axes,[19–22] whereas in the parallel direction no order exists. It is a mesomorphic type of chain aggregation, an intermediate between crystalline and amorphous phases. Therefore, these regions are frequently called paracrystalline ones. When only this type of order exists in a sample, its WAXS pattern contains only reflections related to the lattice planes parallel to the chains axes, that is, with Miller indices of the (*hk*0) type. As one can see in Figure 4, this is the case for fibers without Hap.

However, PAN can also form a completely crystalline structure,[17,22–24] as confirmed by the existence of crystalline lamellae and spherulites in the solid state of PAN. Only in such cases can some reflections related to the lattice planes, which are nonparallel to the chain axes, appear in the WAXS patterns. The third Miller index (*l*) for such planes is non-zero. As one can see in Figure 1, a reflection of this type is clearly visible in the WAXS curve of the PAN H1 sample at the scattering angle of $2\theta \approx 31.9°$. The same reflection is visible in WAXS curves of all remaining samples containing Hap. This fact proves that in all samples with nanoadditives, the mesomorphic structure, which is present in the reference sample PW1, is transformed into a more ordered, typically crystalline structure. This also means that the presence of nanoadditives causes the macromolecular chains to become ordered in the direction parallel to their axes. Most likely, the ordering occurs because of epitaxial growth of PAN crystallites on the Hap grains.

Other evidence in support of a positive influence of the nanoadditive on the crystalline structure quality of the investigated fibers results from the analysis of the angular position of the highest crystalline peak in WAXS patterns, which is related to the family of (110) lattice planes. For the PW1 sample with no Hap, this peak is located at the lowest 2θ value. For the samples containing the nanoadditive, this angle is noticeably higher and slightly but systematically increases with the increasing crystallinity of the sample (Table I). According to Bragg's law, an increase in the peak position indicates a decrease in the average interplanar distance (d_{110}) and consequently an increase in the degree of packing of macromolecules in a crystallite. This means that the density of the crystallites increases. Figure 5 shows the d_{110} values calculated for all samples. The described effect remains in full agreement with the interpretation previously presented. An increase in the density of ordered regions in PAN fibers is related to the transformation of the mesomorphic structure into a crystalline structure. The decrease in d_{110} with an increase in the degree of crystallinity, which can be observed for the group of fibers including Hap, results from the fact that fibers of higher crystallinity contain more crystallites of a better ordered, modified structure. To such a crystalline structure are connected higher strength properties increased to the level of 38 cN/tex. This property increase is in accordance with the demands formulated for precursor fibers and also those that are destined for manufacturing carbon fibers for medical applications, as an exact correlation exists between the crystalline structure and tenacity of the precursor fibers and the tenacity of carbon fibers obtained from them.[10]

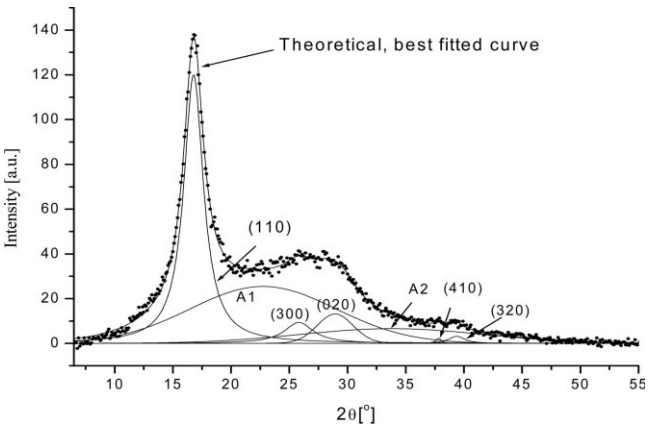

Figure 4 WAXS patterns of the PW1 sample without Hap resolved into crystalline peaks and amorphous maxima. The black points are the experimental curve after normalization and background subtraction. A1 and A2 are amorphous maxima.

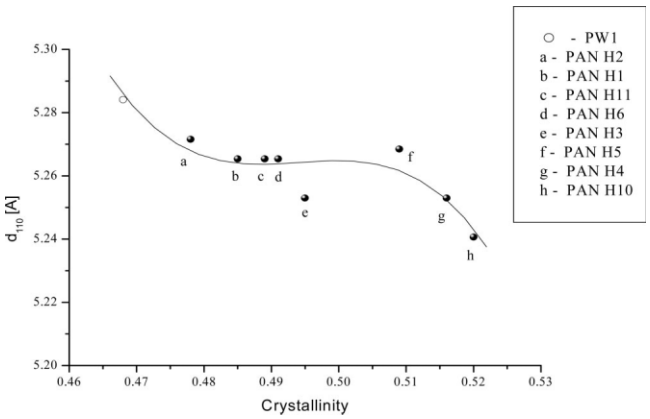

Figure 5 d_{110} for the investigated samples as a function of their crystallinity.

In the case of the overall orientation determined by the sonic method, the basis of its determination is the reference of the velocity of sonic wave propagation in the examined fiber to that in unoriented fiber. Even though the changes in the total orientation are only within the range of 0.59–0.66, in light of the whole range of technological parameters, they also have a significant influence on the tenacity value. The slight increase in the total orientation, which was observed by us while working with more negative values of the as-spun draw ratio and at the same time with higher values of the total draw ratio (Fig. 6), is consistent with the accepted principle of spinning high-tenacity fibers by the wet-spinning-from-solution method.[10] Fibers made under these conditions show the highest values of tenacity. It is also known that the value of the total orientation is considerably affected by pores and empty spaces inside the fibers, which decrease significantly the velocity of sonic wave propagation and result in decreasing the total orientation. This has been confirmed by our previous studies[12] of the porous structure of PAN fibers containing nano-Hap, for which it was found that fibers spun with extremely low as-spun draw ratios showed a total pore volume of 0.125 cm^3/g. On the other hand, fibers spun with increasing positive values of the as-spun draw ratio showed increased total pore volume up to 0.26 cm^3/g. Moreover, the incorporation of nano-Hap into PAN fibers considerably decreases their total orientation (Table II), in contrast to the influence on the degree of crystallinity. This may be connected to the susceptibility of Hap to form agglomerates.

The PAN fibers prepared by us, which include non-fiber-forming additions, show high values of tenacity (Table II). The change in the as-spun draw ratio toward more negative values is accompanied by increasing fiber tenacity, and this is consistent with the trend of changes in the total orientation. Its value depends on the basic technological parameters, that is, the as-spun draw ratio and the total draw ratio (Fig. 6). In general, however, despite the presence of non-fiber-forming nano-Hap in the polymer, these fibers show increased values of tenacity of 31–38 cN/tex. Their tenacity is higher by about 12 cN/tex than that of PAN fibers containing nanosilica, and in the extreme case (sample H5), it is similar to the values obtained for fibers without nanoaddition, such as sample PW1.[11] Lower strength properties of PAN fibers with nano-Hap, in comparison with fibers without nanoadditives, despite the advantageous influence on the crystalline structure, may be connected to the trend toward agglomeration, which in turn is connected with the generation of structural defects.

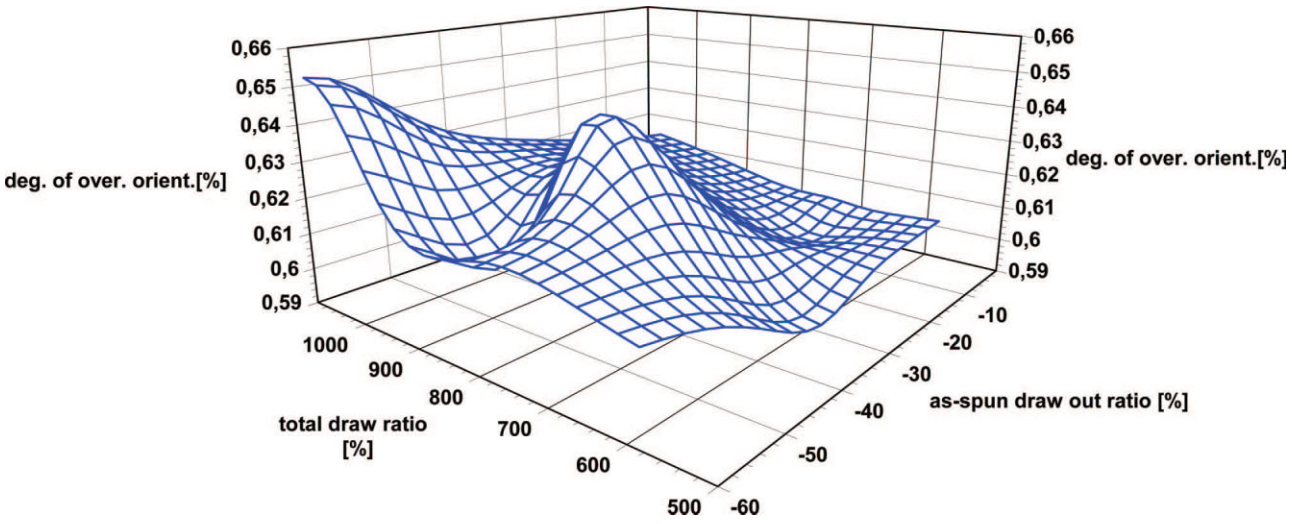

Figure 6 Dependence of the degree of overall orientation on the as-spun draw-out ratio and total draw ratio for PAN fibers containing Hap. [Color figure can be viewed in the online issue, which is available at www.interscience.wiley.com.]

TABLE II
Properties of PAN Fibers with and without Nanoaddition

Sample[a]	As-spun draw-out ratio (%)	Total draw ratio (%)	Total pore volume (cm^3/g)	Crystallite size (Å)	(110) peak position (°)	Degree of crystallinity (%)	Degree of overall orientation	Tenacity (cN/tex)
PAN H5	−60	1074.0	0.125	49.8	16.88	50.9	0.65	43.61
PAN H1	−50	887.6	0.253	48.2	16.83	48.5	0.60	38.19
PAN H6	−40	817.0	0.239	47.8	16.84	49.1	0.64	35.47
PAN H2	−30	583.9	0.232	48.0	16.82	47.8	0.59	27.02
PAN H3	−10	717.3	0.188	48.5	16.87	49.5	0.60	31.18
PAN H4	0.0	765.9	0.264	48.6	16.88	51.6	0.60	33.06
PAN H10	−40	1014.5	-	48.2	16.92	52.0	0.66	38.66
PAN H11	−40	1022.2	-	47.7	16.84	48.9	0.64	39.66
PW1	−40	1054.0	0.071	43.5	16.78	46.8	0.72	47.02

[a]PAN H1 to PAN H6 were fibers formed in a coagulation bath of 60% DMF at 15°C, PAN H10 was fibers formed in a coagulation bath of 60% DMF at 7°C, PAN H11 was fibers formed in a coagulation bath of 60% DMF at 10°C, and PW1 was PAN fibers without nanoaddition formed in a bath of 60% DMF at 15°C.

CONCLUSIONS

The presence of nano-Hap in fiber-grade polymer matter is connected with an increase in the degree of crystallinity and the crystallite dimensions, as well as the transformation of the mesomorphic phase existing in fibers without nanoadditives, in a crystalline structure. This results in an increase in the strength of precursor fibers, which is advantageous for the strength properties of carbon fibers.

The fiber strength properties depend significantly on the as-spun draw ratio and the deformation during the drawing stage. These properties are the outcome of changes in the supermolecular and macroscopic structure of the fiber polymer matter, which depends on the technological process parameters as well as the influence of the nanoadditives in the composite obtained. Suitable control of the process parameters enables obtaining a structure of precursor fibers, which would be appropriate for medical applications of the resultant carbon fibers.

Despite the inclusion of non-fiber-forming nanoadditives in the polymer matter of precursor PAN fibers, which stimulate an increase in the polymer's crystallinity, the fibers are characterized by strength properties significantly higher than the assumed level of 25 cN/tex. This feature predisposes these fibers to obtaining carbon fibers, which would support bone reconstruction, the presence of calcium and phosphorus in the fiber matter being taken into consideration.

The authors thank S. Błażewicz (Academy of Mining and Smelting Engineering, Krakow, Poland) for providing nano-Hap.

References

1. Hehl, G.; Kinzl, L.; Reichel, R. Chirurg 1997, 68, 1119.
2. Campbell, A. C.; Rae, P. S. Ann R Coll Surg Engl 1995, 77, 349.
3. Górecki, A.; Kuś, W.; Błażewicz, S.; Powroźnik, A. Chir Narz Ruchu Ortop Pol 1990, 2, 131.
4. de Groot, K. Rev Ceram Int 1993, 19, 363.
5. Stoch, A.; Długoń, E.; Jastrzębski, W.; Trybalska, B.; Wierzchoń, T. Inż Biomater 2004, 38, 164
6. Szafran, M.; Boryk, E.; Bereza, M.; Parzuchowski, P. Inż Biomater 2004, 38, 150
7. Papkow, S. P. Chim Wołok 1981, 4, 13.
8. Mikołajczyk, T.; Krucińska, I.; Kamecka-Jędrzejczak, K. Text Res J 1989, 59, 557.
9. Mikołajczyk, T.; Krucińska, I. Fibres Text Eastern Eur 1995, 3, 44.
10. Mikołajczyk, T. Scientific Bulletin of the Technical University of Lodz 781, 1997, Scientific Thesis Z 243; Technical University of Lodz: Lodz, Poland.
11. Mikołajczyk, T.; Boguń, M.; Kowalczyk, A. Fibres Text Eastern Eur 2005, 3, 30.
12. Mikołajczyk, T.; Boguń, M. J Appl Polym Sci, 2005, 100, 2881.
13. Mikołajczyk, T.; Boguń, M. Fibres Text Eastern Eur 2005, 1, 28.
14. Błażewicz, S.; Mikołajczyk, T.; Powroźnik, A.; Bogún, M.; Kurzak, A.; Stamińska. Pol. Pat. P-377-921 (2005).
15. Rabiej, M. Polimery 2002, 47, 423.
16. Rabiej, M. Polimery 2003, 48, 288.
17. Stefani, R. Compt Rend 1960, 251, 2174.
18. Brandrup, J.; Immergut, E. H.; Grulke, E. A. Polymer Handbook; Wiley: New York, 1999.
19. Kitajgorodskij, A. J. Dokl Akad Nauk 1959, 4, 861.
20. Natta, J.; Mazanti, J.; Corradini, P. Atti 1960, 25, 3.
21. Urbańczyk, G. Scientific Bulletin of the Technical University of Lodz 45; Technical University of Lodz: Lodz, Poland, 1962; p 79.
22. Klement, J. J.; Geil, P. H. J Polym Sci Part A-2: Polym Phys 1968, 6, 1381.
23. Patel, G. N.; Patel, R. D. J Polym Sci Part A-2: Polym Phys 1970, 6, 1381.
24. Hinrischen, G.; Orth, H. Kolloid Z Z Polym 1971, 247, 844.